

## Dual Stabilization Heat Treatment in a TRIP Assisted Steel to Realize Third Generation Advanced High Strength Steel Properties

J N Mohapatra\*, D Satish Kumar, G Balachandran

Research and Development, JSW Steel Limited, Vidyanagar, Toranagallu, Karnataka, India

### ABSTRACT

Low carbon steel (0.17 wt. % C) with 1.72% Mn and 1.35% Si, micro alloyed with 0.02% Nb and 0.04% Ti was subjected to dual stabilization heat treatment that involves intercritical austenitization at 790 °C, 810 °C and 830 °C for 5 minutes for first stabilization followed by isothermal bainitic holding at 450 °C for 30 seconds and water quenched to form martensite and retained austenite. The steel was reheated to 450 °C for 30 seconds, where partition of carbon from martensite to retained austenite take place stabilizing the austenite second time and then water quenched. The steel showed 45% to 47% ferrite, 21%-37% bainite, 14% to 26% martensite and 3.3% to 9.5% retained austenite. The mechanical properties showed yield strength between 460 and 480 MPa, tensile strength between 960 and 1010 MPa, total elongations between 27 and 28% with tensile toughness above 27 GPa.% conforming to third generation advanced high strength steel.

**Keywords:** Low carbon steel; Dual stabilization heat treatment; Microstructure; Mechanical Properties; Third gen advanced high strength steels

### INTRODUCTION

There are several different mechanisms by which third generation advanced high strength steels are produced. The development of such steels ensures light weight structure with good energy absorption or formability characteristics. The steels include fine grained DP steel, high ductility DP steel, Ferrite-Bainite steel, TRIP Steel, Quench and Partitioned type steels and tempered martensite type steels. One of the other mechanisms for the development of such steel is called the dual stabilization heat treatment. Not many published information is available on the process. The TRIP assisted steels, in general responds to the dual stabilization heat treatment Two steels with a base composition 0.3% C, 0.5% Cr and 4% Mn, one with 1.8% Si and 0.6% Al while the other one with 2.1% Si and 1.5% Al was subjected to dual stabilization heat treatment reported earlier [1]. The elements Al and Si suppress carbide formation and promote retained austenite. The processing involves austenitization at 900 °C and 835 °C followed by isothermal bainitic holding briefly followed by quenching between 80 °C to 125 °C to form martensite. This is followed by reheating to isothermal bainitic condition where carbon gets partitioned. The phase constitution involves more than 30% retain austenite along with bainitic ferrite and martensite. The first steel had a tensile strength in the range 1100 to 1450 MPa and total elongation in the range 8% to 14%, and the second steel has tensile strength from 1400 to 1650 MPa and total elongation from 16% to 22%. Dual stabilization where initially the first stabilization takes place in the intercritical temperature range [2]. The second stage is a single stage quench partition treatment, where there is martensite formation during quenching and the carbon

partitioning takes place during higher temperature isothermal holding. The steel has a composition (wt.%) of 0.11% C, 1.5% Mn, 1.16% Si, 0.043% Al, 0.024% Cr, 0.01% Ti, 0.001% S, 0.008% P, and 0.003% B. The properties realized shows 875 to 910 MPa tensile strength with 20% to 24% elongation respectively and the tensile toughness was 21 GP. Physical simulation and dilatometric study of double step heat treatment of medium manganese steel with composition of 3.3 wt.% Mn, 0.17 wt. % C, 1.6 wt.% Al, 0.23 wt.% Mo and 0.22 wt % Si is reported with a bainitic structure and high volume fraction of residual austenite and hardness of 370 Hv [3], however alloying addition in the steel increase the cost of production and need to be taken care. The objective of the present study is to develop third generation Advanced High Strength (AHSS) properties in a lean alloyed TRIP assisted steel by the dual stabilization heat treatment and understand the structure and properties evolution in the thermal cycle adopted.

### MATERIALS AND METHODS

The steel used for the present study was made in JSW Steel Ltd., Vijayanagar Works of 3 mm hot rolled product. The chemical analysis of the steel was carried out using optical emission spectroscopy of SPECTRO Make. Samples of the steel strip were subjected to heat treatment as per the cycle shown in Figure 1. The heat treated samples were subjected to microstructural analysis using Nital and Picral etchants for optical metallographic investigation. The optical microscopy was carried out using Olympus Make opto-digital microscope. The SEM analysis was performed using Hitachi Make SEM unit. The phase analysis using optical microscopy by etching with

**Correspondence to:** JN Mohapatra, Research and Development, JSW Steel Limited, Vidyanagar, Toranagallu, Bellary-583275, Karnataka, India, E-mail: jitendra.mohapatra@jsw.in.

**Received:** 26-Aug-2022, Manuscript No. AAE-22-18284; **Editor assigned:** 01-Sep-2022, PreQC No.AAE-22-18284 (PQ), **Reviewed:** 19-Sep-2022; QC No. AAE-22-18284, **Revised:** 27-Sep-2022, Manuscript No.AAE-22-18284 (R); **Published:** 03-Oct-2022, DOI: 10.35248/2167-7670.22.11.201

**Citation:** Mohapatra JN, Kumar DS, Balachandran G (2022). Dual Stabilization Heat Treatment in a TRIP Assisted Steel to Realize Third Generation Advanced High Strength Steel Properties. J Adv Automob Eng. 11:201.

**Copyright:** © 2022 Mohapatra JN, et al. This is an open-access article distributed under the terms of the Creative Commons Attribution License, which permits unrestricted use, distribution, and reproduction in any medium, provided the original author and source are credited.

Nital and Lepera etchant showed fine phase features and the usage of optical image analysis on such a fine structure gave erroneous results for the phase fraction. Hence, SEM micrographs were used for the phase analysis. The individual phases were clearly seen in SEM micrographs. The ferrite phase is the matrix gray phase, martensite is flat structure without carbides, the bright white rim portion of the martensite or within bainite zone is the retained austenite. Cementite can also be bright white, but here all the bright white filmy phases were taken as retained austenite. Granular dispersion of particulates was taken as bainite. For every condition two SEM micrographs were acquired. Although it is a micro area examination than optical, the features covering uniform region was taken. A 10 × 10 grid was used and the phases were assessed by manual counting. At least 3 measurements were carried out in each micrograph and an average phase fraction was obtained from the 6 sets of reading. XRD analysis using PAN alytical XRD machine was conducted on the samples to evaluate the retained austenite volume fraction. The mechanical properties were determined on the samples at various heat treated conditions. Tensile samples were made as per ASTM E8M subsize specimens. The tensile test was carried out using Zwick/Roell make 250 kN tensile testing machine at a strain rate of 0.008/s. Thermocalc (Version-2020b) software was used for the evaluation of the pseudo-binary phase diagram to assess the phase fields with temperature as a function of carbon content as shown in Figure 2.

which enhances the austenite field and promotes more austenite at lower austenitization temperatures. The steel has 1.35% Si which suppresses the carbide formation during austempering and promotes the formation of austenite by inhibiting the carbide nucleation. The steel has 0.04% Ti and 0.06% Al which fixes the nitrogen content in the steel. The residual Ti and Nb tend to form carbides as well. The nitrides and carbides in the steel tend to restrict the grain growth and ensure formation of fine grained steel. The transition temperatures shown in Table 1 were evaluated using Cambridge University software (MUCG83) [4]. The heat treatment carried out involves, an initial intercritical holding, where carbon partitioning takes place. The amount of ferrite content increases, as the inter critical austenitization decreases. The intercritical treatment further tends to partition the carbon between the ferrite and equilibrium austenite. As the ferrite phase has low solubility, the carbon rejected by the ferrite phase formation tends to enrich the austenite phase. As the carbon content of the austenite increases, there is higher tendency for the carbon to decrease the MS temperature and at sufficiently higher carbon content the austenite is stabilized. This stage is the first stage stabilization of the austenite. There are several possibilities to enhance the carbon stabilization along with the next stage of phase transformation. This second stage also results in retained austenite that gets enriched with the carbon rejected by other phases that provides the second stabilization. The second stage stabilization has various possibilities that include, direct quench or step quench the steel to BS temperature and before bainite starts transforming, quench to below MS Temperature and follow a single stage quench partitioning. Both tends to form martensite and retained austenite, the fraction of which can be controlled by the choice of the quench temperature as determined by Koinstein-Maurberger equation. The quenching may be followed by a single stage quench partitioning or a dual stage quench partitioning. The second stage may be below the MS temperature or between MS and BS temperature. Directly quench the steel to isothermal bainitic holding range where a certain amount of bainitic transformation takes place. During this transformation, the steel is quenched to convert the residual austenite during bainitic transformation. The residual austenite transforms to martensite and retained austenite. Hence, microstructure has ferritic bainite or carbide free bainite initially followed by martensite and retained austenite. Thus, it is seen that all the above variants are mentioned in literature. It is also seen that such treatments are good for high Mn steels [2], which enables Mn partition during the first stage stabilization. In the present study, the intercritical treatment was followed by a two stage quench partitioning as the second stage stabilization. In the present case, when the steel is subjected to inter critical treatment at 790 °C, 810 °C and 830 °C, using Lever rule in phase diagram in Figure 2, the equilibrium austenite content was estimated from the phase diagram to be 43%, 53% and 71%, the rest being intercritical ferrite. As the carbon solubility of ferrite is 0.02%, the carbon rejected by ferrite fraction enriches the austenite fraction. The carbon content of austenite was estimated to be 0.36%, 0.29% and 0.23% respectively at 790 °C, 810 °C and 830 °C. After a brief step quenching to 450 °C for 30 seconds, simulating a galvanized bath, the steel was quenched to room temperature. The austenite fraction transforms to martensite and retained austenite which was estimated using Koinstein-Maurberger equation.

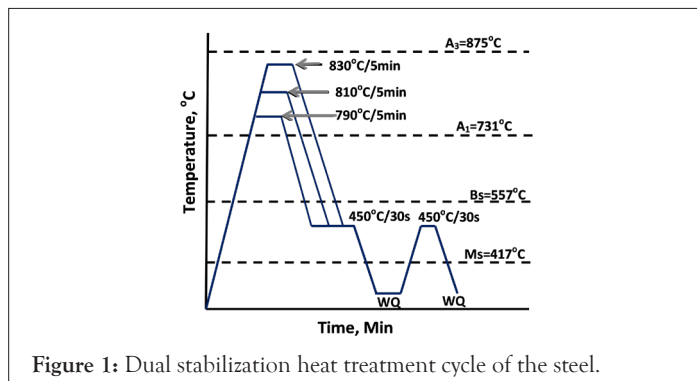


Figure 1: Dual stabilization heat treatment cycle of the steel.

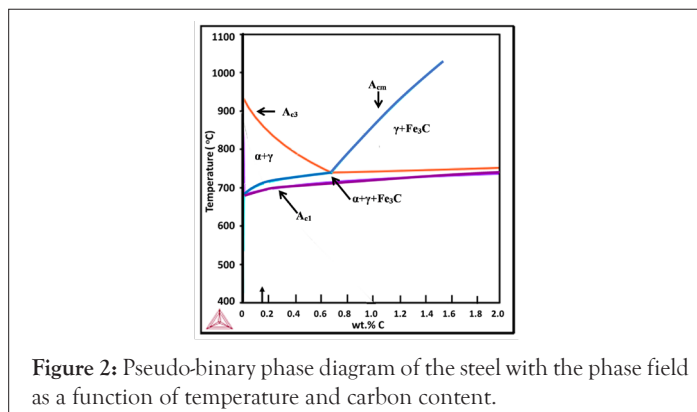


Figure 2: Pseudo-binary phase diagram of the steel with the phase field as a function of temperature and carbon content.

## RESULTS AND DISCUSSION

The chemical composition of the steel is shown in Table 1. The composition of the steel used is a TRIP assisted steel with 0.17% C, good for weld ability and formability. The steel has 1.7% Mn content

Table 1: Chemical composition of the steel (wt.%).

C	Mn	Si	Nb	Ti	N	Al	S	P	AC1	AC3	Bs	Ms
0.17	1.72	1.35	0.02	0.04	0.005	0.06	0.003	0.016	731	875	557	417

$$FM(\%)=(1-e \{-0.011(MS-QT)\}) \quad (1)$$

Where FM=Martensite Fraction at the quench temperature. QT is the quench temperature which is room temperature and MS is the martensite start temperature. The fraction of martensite is 98% of the inter critical austenite. And the carbon content of the austenite is increased with the increase in inter critical ferrite content due to partitioning of the carbon. The optical microstructure of the samples made using Nital and Lepera etchants is shown in Figure 3. The Nital etching clearly brings out the inter critical blocky ferrite along with other phases. The Lepera etchants show both bainite and martensite features etched together. Estimating of individual phases was becoming difficult due to the finer structure. Hence, SEM micrographs where the individual phases became resolvable were taken for the phase estimation. The SEM micrograph (Figure 4) shows gray intercritical ferrite phase. The martensitic phase was featureless and the bainitic phases are regions with bright carbides. The rim of the martensite zone and the streaky bright white film portion was considered as retained austenite for manual estimation. A  $10 \times 10$  optical grid was used on the SEM micrographs, and in two representative images 3 sets of reading were taken on each micrograph and the average of each phase was estimated. The SEM images in Figure 4 show both lower and higher magnification. The lower magnification shows blocky regions of inter critical ferrite. The inter critical ferrite content is more in  $790^\circ\text{C}$  austenitized sample and it decreases with increasing austenitization temperature. In the higher magnification micrographs other phases are visible. The bright white films of retained austenite are seen engulfing the martensite zones. The actual phase estimated using SEM analysis is shown in Table 2. XRD analysis was performed in the sample and the retained austenite as measured by XRD analysis shows in the range of 3.32% to 9.45% while the manually measured retained austenite was much higher. This may be due to the carbide being counted in place of retained austenite which also shows similar appearance in the SEM images. The data in Table 2 is realistic in terms of ferrite and martensite contents, while the bainite value can be corrected with XRD phase analysis for retained austenite. The theoretical estimation of phases was carried out, which is at variance with the actual phase analysis as shown in Table 3. The intercritical ferrite content was estimated by applying the phase rule in the intercritical region in the phase diagram. The ferrite and austenite content was estimated. The formation of ferrite partitions the carbon from ferrite to austenite and the carbon enriched austenite decreases its MS Temperature. This is the first stabilization. In the second stage, the steel is quenched to water after a very brief holding at  $450^\circ\text{C}$ . This creates a quenching treatment using equation (1) enables estimation of the formation of martensite and the residual retained austenite during quenching. The estimated retained

austenite by this method shows much lower retained austenite than the actual retained austenite measured using XRD. Such discrepancies are reported in quench partition literature [5]. XRD of the final steel subjected to Dual stabilization heat treatment showing increasing retained austenite content with decreasing intercritical austenitization temperature (Figure 5). The mechanical properties of the steel are given in Table 4. It is seen that the steel responds to dual stabilization treatment with ultimate tensile strength range between 965 to 1007 MPa with corresponding elongation between 27% and 28%. The yield ratio of the steel is 0.47 to 0.5. This implies that the steel is further formable or it can absorb energy on impact by deformation. The tensile toughness consistently around 27 GPa.%. The variation in strength and toughness with austenitization condition is not significant. This may be attributed to the uniform equilibrium phases attained post quenching and isothermal holding at  $450^\circ\text{C}$ . At this stage other than the stable retained austenite the other phases are ferrite, bainite and tempered martensite. Engineering stress-strain diagram of the steel after Dual stabilization heat treatment (Figure 6).

The work hardening behavior of the steel was assessed by Hollomon equation;

$$\sigma = K \varepsilon^n$$

Where  $\sigma$  and  $\varepsilon$  are true stress and true strain and  $n$  is the strain hardening exponent. The work hardening behaviour shows two distinct slopes as shown in Figure 7. The modified Crussard-Jaoul (CJ) model [6] was also applied to understand the work hardening behavior as shown by;

$$\text{Where, } \varepsilon = \varepsilon_0 + c\sigma^m$$

$\varepsilon_0$ =initial true strain,  $m$ =strain hardening index and  $c$  is a constant. In a differential form;

$$\ln(d\sigma / d\varepsilon) = (1-m)\ln\sigma - \ln(cm)$$

The result for the modified C-J model is shown in Figure 8. The work hardening may be treated in two distinct regimes. In both the work hardening models (Figures 7 and 8) the work hardening rate increases as dislocation movement take place in the polygonal ferrite phase initially and it is followed by simultaneous deformation of polygonal ferrite along with harder tempered martensite phases and retained austenite phases. Finally, the dislocation pile-up, immobilization and void nucleation towards cracking takes place. The  $n$  value is lower to start with and it increases beyond a critical level where the  $n$  value increases [7,8]. The  $n$ -value calculated by the two models show some variations as in Table 5 and depends on where we assess the slope.

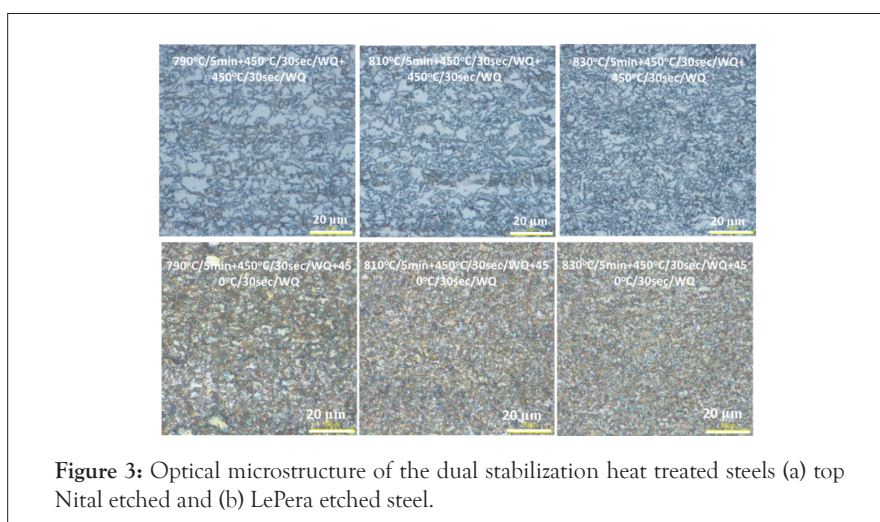


Figure 3: Optical microstructure of the dual stabilization heat treated steels (a) top Nital etched and (b) Lepera etched steel.

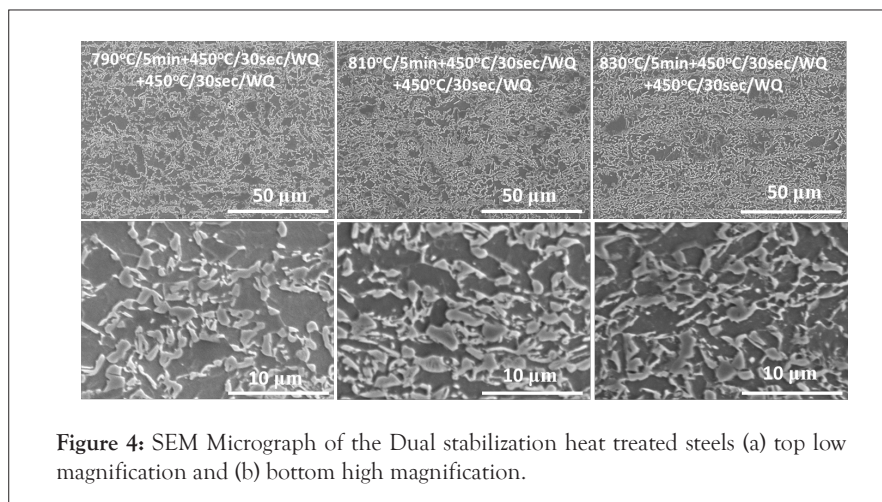


Figure 4: SEM Micrograph of the Dual stabilization heat treated steels (a) top low magnification and (b) bottom high magnification.

Table 2: Phase fraction evaluation by SEM phase analysis.

Heat treatment condition	SEM measured % ferrite	SEM measured % martensite	SEM % retained austenite	SEM measured % bainite	% Retained austenite by XRD
790	66	18.5	10	5.5	9.45
810	52	24	12	12	6.78
830	43	17	11	29	3.32

Table 3: Theoretical Phase analysis of the dual stabilization heat treatment.

Intercritical temperature	Intercritical austenite %	Intercritical ferrite%	% Carbon in intercritical austenite	Ms (°C)	Quench temp (°C)	Calculated martensite* %	Calculated austenite %	Actual austenite by XRD analysis
First stage stabilization			Second stage stabilization					
790	43	57	0.36	325.8	25	41.43	1.57	9.45
810	53	47	0.29	355.4	25	51.6	1.4	6.78
830	71	29	0.23	380.8	25	69.58	1.42	3.32

Note: \* Using Koinsteinen-Maurberger equation.

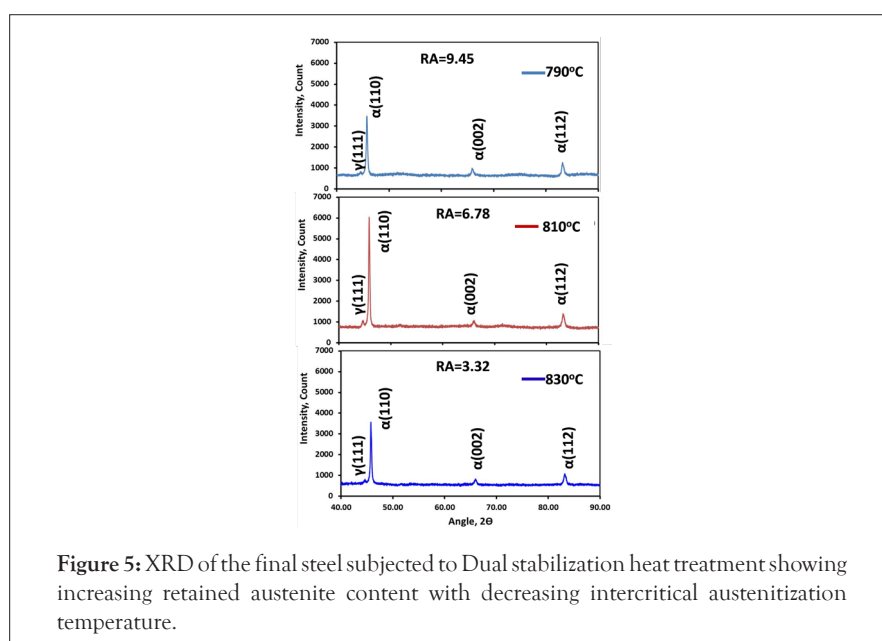
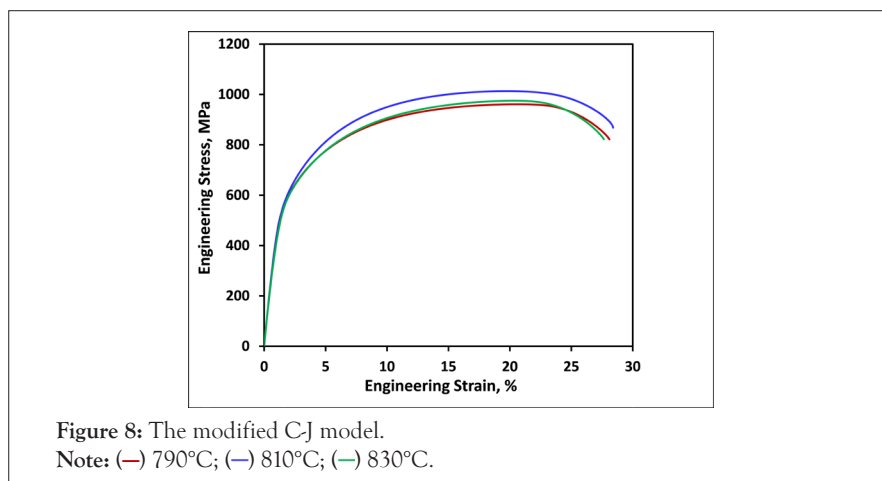
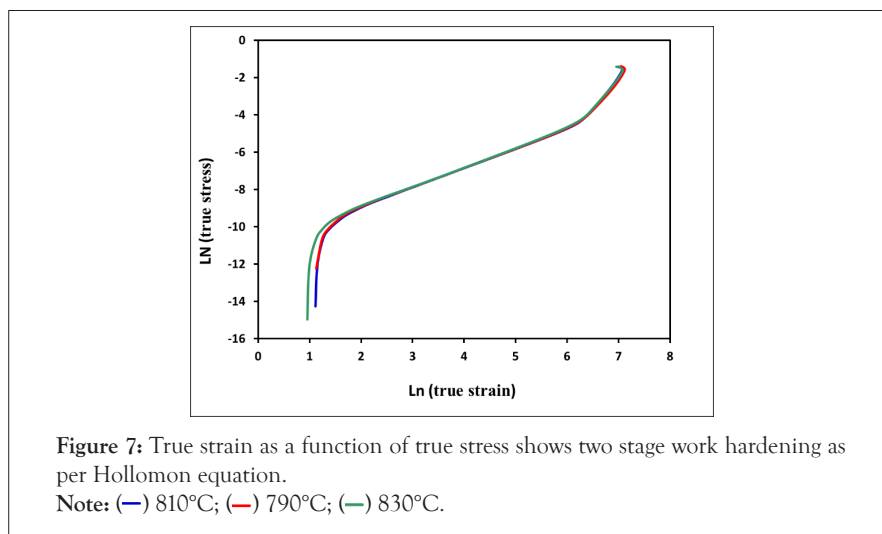
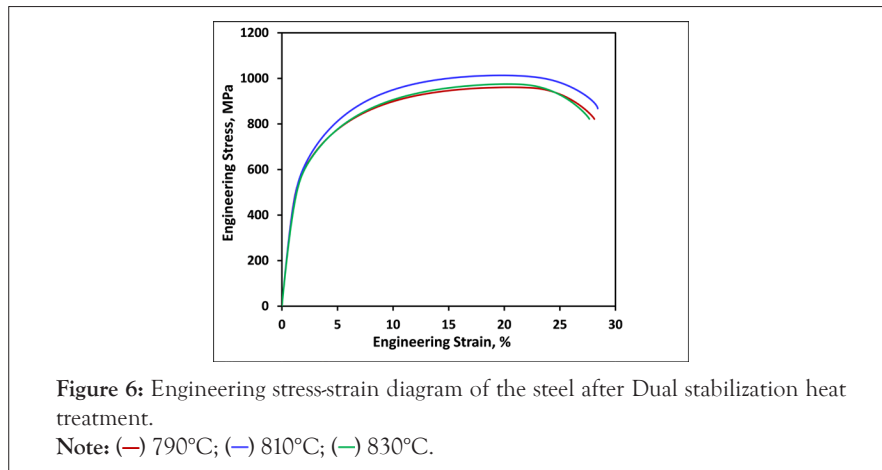


Figure 5: XRD of the final steel subjected to Dual stabilization heat treatment showing increasing retained austenite content with decreasing intercritical austenitization temperature.

Table 4: Mechanical properties of the steels.

Dual stabilization heat treatment condition	YS (0.2%)Mpa	UTS MPa	TE%	YR	UTS × TE GPa.%
790°C/5min+450°C/30 sec+WQ+450°C/30 sec+WQ	461 ± 13	979 ± 4	27.7 + 0.015	0.47	27.12
810°C/5min+450°C/30 sec+WQ/450°C/30sec+WQ	474 + 6	1007 ± 6	27.4 + 1	0.47	27.59
830°C/5min+450°C/30sec+WQ/450°C/30sec+WQ	484 ± 1	965 ± 3.5	28.1 + 0	0.5	27.1



**Table 5:** Analysis of two distinct slopes in the work hardening models.

Slope	790 °C/5 min+ 450 °C/30 sec/WQ +450 °C/30sec/WQ		810 °C/5 min +450 °C/30 sec/WQ +450 °C/30sec/WQ		830 °C/5 min +450 °C/30 sec/WQ +450 °C/30sec/WQ	
	CJ Model	Hollomon	CJ Model	Hollomon	CJ Model	Hollomon
(1-m)	-3.02	-	-2.87	-	-3.06	-
m	4.02	-	3.87	-	4.06	-
n1	0.25	0.36	0.26	0.34	0.25	0.34
(1-m)	-8.83	-	-4.69	-	-12.62	-
m	9.83	-	5.69	-	13.62	-
n2	0.1	0.24	0.18	0.27	0.07	0.21

## CONCLUSION

Dual stabilization heat treatment could be applied to lean alloyed steel (0.17% C, 1.35% Si, and 1.73% Mn with micro alloying additive of 0.02% Nb, 0.04% Ti and 0.06% Al) to achieve third generation advanced high strength steel properties. The cycle involves intercritical austenitization between 790 °C to 830 °C for 5 minutes for first stage carbon partitioning towards stabilizing the retained austenite. This was followed by brief isothermal holding at 450 °C for 30 seconds to simulate galvanizing condition. This is followed by second stage stabilization involving a two stage quench partitioning where quenching takes place to room temperature followed by a partitioning at 450 °C isothermal holding. The final microstructure of the steel consists of 45% to 47% ferrite, 21% to 37% bainite, 14% to 26% martensite and 3.3% to 9.5% retained austenite. The steels with the said treatment showed almost similar properties at all different austenitization temperatures. The mechanical properties showed yield strength between 460 and 480 MPa, tensile strength between 960 and 1010 MPa, total elongations between 27% and 28% and tensile toughness above 27 GPa % conforming to third generation advanced high strength steel.

## REFERENCES

1. Qu H, Michal GM, Heuer AH. Third generation 0.3 C-4.0 Mn advanced high strength steels through a dual stabilization heat treatment: austenite stabilization through paraequilibrium carbon partitioning. *Metall Mater Trans A*. 2014;45(6):2741-2749.
2. Jing C, Ding X, Ye D, Zhao J, Lin T, Xu S. Effect of Different Isothermal Time on Microstructure and Mechanical Property of the Low-Carbon Steel Treated by Dual-Stage C-Mn Partitioning Process. *Scanning*. 2020.
3. Skowronek A, Morawiec M, Ruiz-Jimenez V, Garcia-Mateo C, Grajcar A. Physical simulation and dilatometric study of double-step heat treatment of medium-Mn steel. *Arch Civ Mech Eng*. 2020;20(4):1-1.
4. Mohapatra JN, Kumar DS, Balachandran G. Development of a Lean Alloyed Trip Assisted Bainitic Steel by Austempering Treatment. *Trans Indian Inst Met*. 2022;75(1):229-238.
5. Speer JG, Assunção FC, Matlock DK, Edmonds DV. The “quenching and partitioning” process: Background and recent progress. *Mater Res*. 2005;8:417-423.
6. Xiong ZP, Kostyrychev AG, Saleh AA, Chen L, Pereloma EV. Microstructures and mechanical properties of TRIP steel produced by strip casting simulated in the laboratory. *Mater Sci Eng*. 2016;664:26-42.
7. Gao G, Bai B, Zhang H, Gui X, Tan Z, Weng Y. Enhanced TRIP effect in lean alloy steel treated by a ‘disturbed’bainitic austempering process. *Heat Treat Surf Eng*. 2019;1(1-2):72-77.
8. Kim J, Chung KH, Lee W, Kong J, Ryu H, Kim D, et al. Optimization of boost condition and axial feeding on tube bending and hydro-forming process considering formability and spring-back. *Met Mater Int*. 2009;15(5):863-876.